

# We are IntechOpen, the world's leading publisher of Open Access books Built by scientists, for scientists

6,900

Open access books available

186,000

International authors and editors

200M

Downloads

Our authors are among the

154

Countries delivered to

TOP 1%

most cited scientists

12.2%

Contributors from top 500 universities



WEB OF SCIENCE™

Selection of our books indexed in the Book Citation Index  
in Web of Science™ Core Collection (BKCI)

Interested in publishing with us?  
Contact [book.department@intechopen.com](mailto:book.department@intechopen.com)

Numbers displayed above are based on latest data collected.  
For more information visit [www.intechopen.com](http://www.intechopen.com)



## Parallel channels using frequency multiplexing techniques

Magnus Karlsson, Allan Huynh and Shaofang Gong  
 Linköping University  
 Sweden

### 1. Introduction

The principle of frequency (de-) multiplexing provides the opportunity to either split a wide frequency-band into several parallel sub-bands or to combine parallel sub-bands into one wide frequency band. A typical de-multiplexing operation is that a wideband signal from a single broadband antenna is divided into sub-bands for parallel data processing. Similarly, several services from a single antenna can be separated utilizing a de-multiplexing technique during reception, and combined with multiplexing during transmission. Moreover, the relation can be the opposite, i.e., a system containing several narrowband antenna can be connected to a single transceiver using the (de-) multiplexing technique. This chapter presents stand-alone components as well as UWB radio front-end configurations, utilizing multiplexing techniques. Implementations are demonstrated both with conventional multi-layer and flex-rigid printed circuit board technologies. Fig. 1 shows the principle of (de-) multiplexing, where FMN is the abbreviation of frequency multiplexing network.

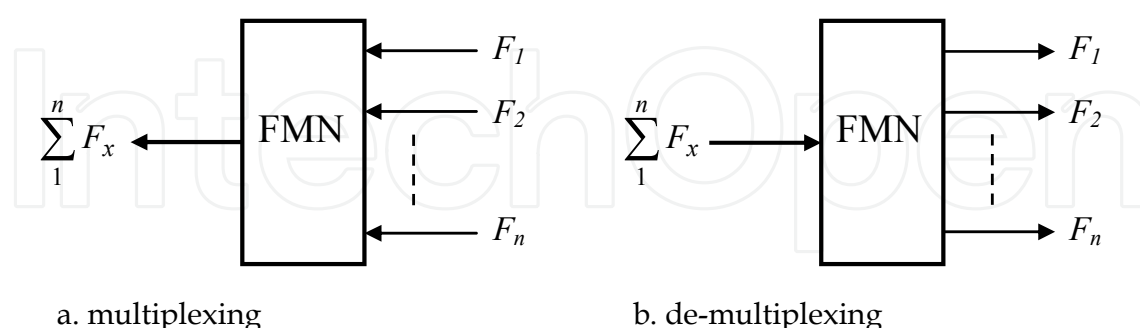


Fig. 1. The principle of frequency (de-) multiplexing.

In multi-band systems, frequency multiplexers are used to replace switches, and for channel parallelism. The concept of multiple frequency channels has been around for roughly half a century. For instance, (Coale, 1958) suggested to use directional filters as basic building blocks for frequency multiplexing, and a waveguide solution for operation in the X-band is

shown as a demonstrator. A few years later (Rhodes & Levy, 1979) presents a generalized manifold theory. In brief terms the manifold (Bandler et al., 1987) presents an optimization algorithm for waveguide multiplexers. The algorithm is demonstrated with a 12-channel narrow-band waveguide multiplexer around 12 GHz. Three sub-bands multiplexed to one common frequency-band is also known as a triplexer, e.g., (Mansour, 1994) demonstrates a triplexer using dual-mode high-temperature superconductor thin-film filters and cryogenic circulators. In general manifolds suffer from the drawback of a large number of network variables that must be solved simultaneously. Various optimization techniques and algorithms to ease design and implementation have been proposed. Utilizing prototype circuits based on infinite-array logarithmic-periodic principles (Rauscher, 1994) showed two multiplexer solutions using transmission lines, resonators and coupling capacitors. (Kirilenko et al., 1994) demonstrates procedures for minimizing the need of experimental correction when using computer-aided design. Waveguide technology is quite common in manifold multiplexers since sharp sub-band filter cut-offs increases neighbouring sub-band to sub-band isolation, i.e., matching the circuitry is easier. A waveguide duplexer and a four-channel multiplexer are designed using electromagnetic simulation. (Matthaei et al., 1996) presents a lumped element and manifold microwave multiplexer using the high-temperature superconductor technology. Classically frequency-multiplexed selection relies on band-pass filtering. Reversing the principle by blocking out of sub-band frequencies using band-stop filters has also been shown. (Bariant et al., 2002) presents a microstrip duplexer using band-stop filters. The band-stop filtering is achieved using open circuit stubs. (Ohno et al., 2005) presents both a duplexer and a triplexer for printed circuit board integration. However, the design still involves some lumped components and the sub-bands are fairly small, having large guard-bands. In reference (Chen et al., 2006) a duplexer using microstrips is presented, but requires structural redesign to extend the number of ports. Paper (Lai & Jeng, 2005) proposes a stepped-impedance multiplexer for UWB and WLAN coexistence. In reference (Mallegol et al., 2007) a narrow-band four-channel multiplexer using open loop resonators for multi-band on-off keying UWB is demonstrated. Papers (Stadius et al., 2007; Tarng et al., 2007) show two channel-select multiplexers intended for UWB local oscillator signal selection, i.e., only one sub-band is active at the time.

## 2. Printed Circuit Board Build-up

Multi-layer printed circuit boards are commonly used to build space efficient electronics. Standard printed circuit board processes can today provide many choices when it comes to material selection and stack build-up techniques. Fig. 2 shows two different alternatives. Fig. 2(a) and (b) show a regular four metal-layer and flex-rigid (four metal-layer in the rigid part, and two metal-layers in the flexible part) printed circuit boards, respectively. In detail Fig. 2(a) is built-up as follows: Two dual-layer Rogers 4350B (RO4350B) boards processed together with a Rogers 4450B (RO4450B) prepreg. RO4450B prepreg is a sheet material (e.g., glass fabric) impregnated with a resin cured to an intermediate stage, ready for one stage printed circuit board bonding. The flex-rigid printed circuit board in Fig. 2(b) is built-up similarly but the choices of material must be such that the rigid contour can be cut out with depth controlled laser milling. Using LF8520, LF0100, LF0110 and AP8525 from DuPont™ Pyralux® laminate series. AP series is polyimide only materials, used for the flexible substrate layer. LF8520 is a combination of polyimide and fully cured adhesives, more

physically stiff than an AP series material. LF0100 is an adhesive used for printed circuit board bonding, while the LF0110 is commonly used as protective coating on flexible substrate layers. The rigid and the flexible substrates are processed together in a printed circuit board bonding process, i.e., the adhesive layers are used to bond the polyimide layers. The flex-rigid technology provides additional possibilities compared to regular boards when it comes to printed circuit board component integration. For instance, the antenna is placed in the flexible part for best connectivity, while the rest of the transceiver is space efficiently built in the rigid part. Moreover, distributed components like a balun or a triplexer can be integrated in the printed circuit board as if the rigid part was a regular four metal-layer printed circuit board.

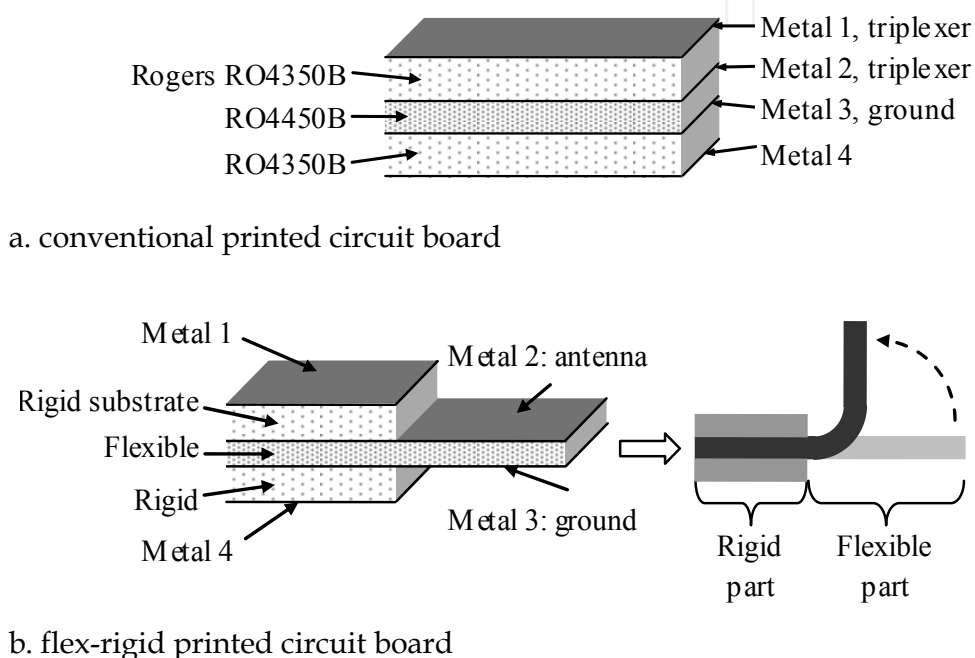
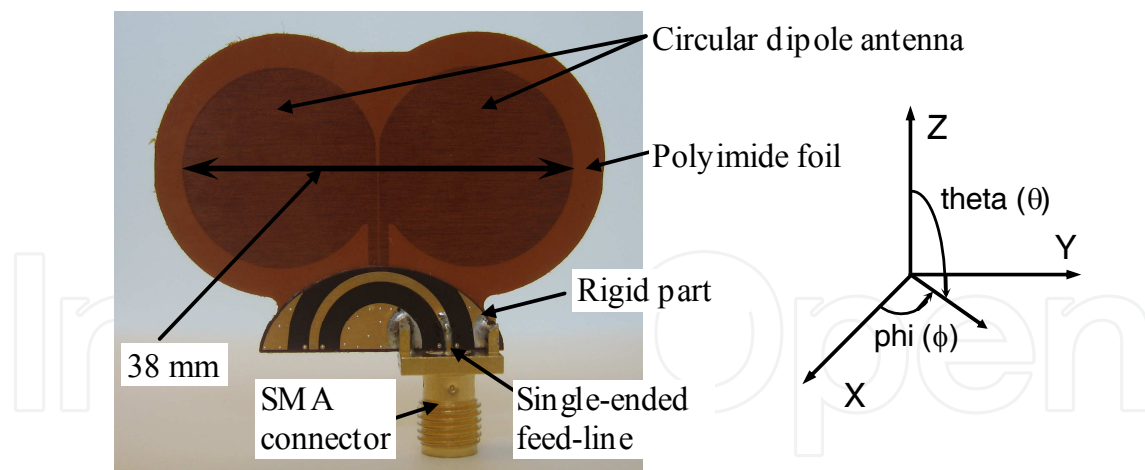


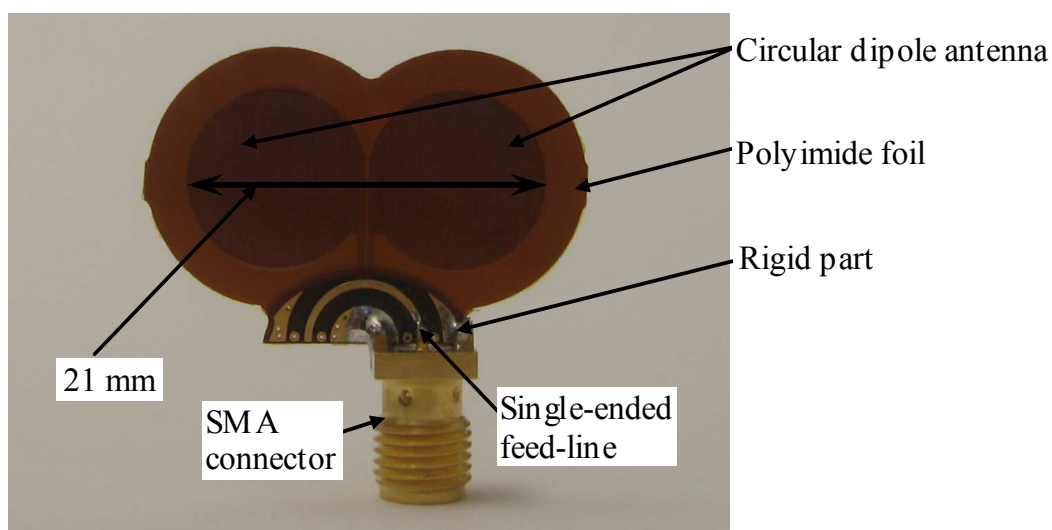
Fig. 2. Printed circuit board structures.

### 3. Circular Dipole Antenna

Fig. 3 shows circular dipole antenna for UWB realized using the flex-rigid substrate. The antenna is positioned in the  $x$ - $y$  plane, and  $\phi=0$  (Horizontal plane) is along the  $x$ -axis. It is seen that the radiating antenna element is placed entirely on the flexible part of the substrate. Furthermore, the balun is integrated in the rigid part of the substrate (Karlsson & Gong, 2008). A balun is needed to convert the differential port of the dipole antenna to a single-ended port, i.e., to connect to a single-ended front-end. The backside of the rigid part (Metal 4) is completely covered with metal to make through-board ground vias possible, and to provide additional solderable ground-junctions for the SMA connector (Karlsson & Gong, 2009). Drilled vias with a diameter of 0.3 mm are used for grounding. For a detailed study of the performance of the Mode 1 antenna, see (Karlsson & Gong, Oct. 2009). Antenna solutions for both the Mode 1 and the 6-9 GHz frequency bands was originally presented in (Karlsson et al., Sept. 2009).



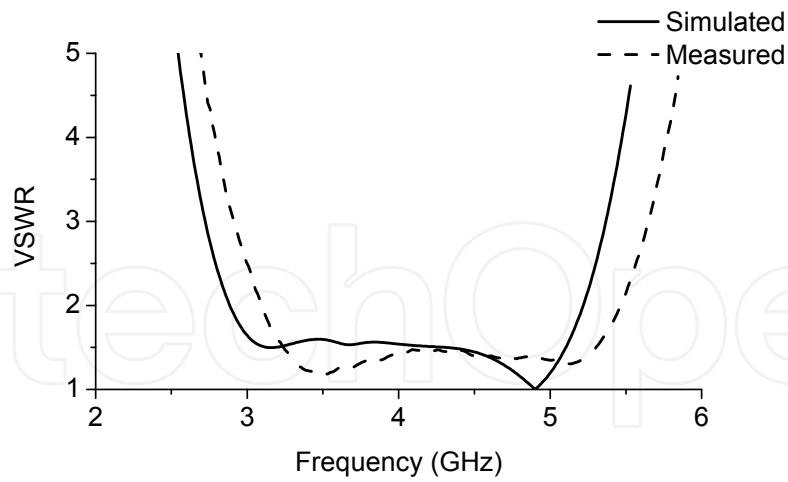
a. Mode 1 UWB antenna



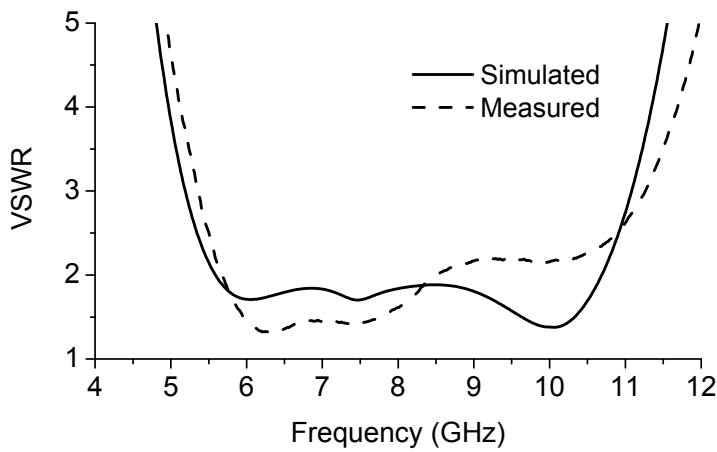
b. 6-9 GHz antenna

Fig. 3. Circular dipole UWB antenna: (a) Mode 1 antenna (3.1-4.8 GHz), and (b) 6-9 GHz antenna.

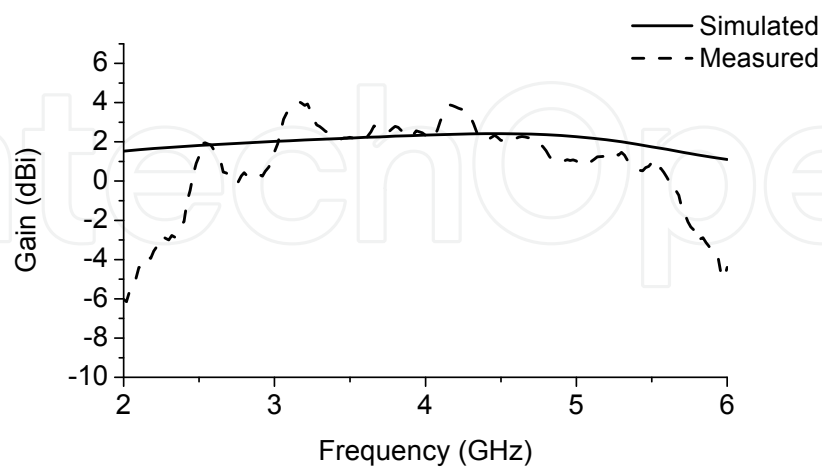
Fig. 4(a) and (b) show voltage standing wave ratio (VSWR) simulations and measurements of the circular dipole antenna on the flex-rigid substrate. The VSWR simulation and measurement results with the balun are shown. It is seen in the simulated and measured results that the circular dipole antenna for the upper UWB band (6-10.6 GHz) has a wide impedance bandwidth (a  $VSWR < 2.5$  bandwidth from 5.5 to 11.0 GHz). A small shift in frequency is also seen in both graphs, which is likely due to the fact that the simulated phase velocity is lower than the actual one (Karlsson & Gong, 2009). Fig. 4(c) shows simulated and measured gain in dBi at the boresight direction of the Mode 1 antenna. A match between simulation and measurement is seen within the Mode 1 UWB frequency-band (3.1-4.8 GHz), and a gain around 2 dBi is observed. However, some difference between simulation and measurement is seen, especially outside the Mode 1 UWB frequency-band. This is also due to the fact that the effect of the balun is not included in the radiation simulation (Karlsson & Gong, 2009).



a. VSWR simulation and measurement of the Mode 1 UWB antenna



b. VSWR simulation and measurement of the 6-9 GHz UWB antenna



c. gain simulation and measurement of the Mode 1 UWB antenna

Fig. 4. Circular dipole antenna simulations and measurements.

## 4. Triplexer

Fig. 5 shows a schematic of a multiplexer with three sub-bands, i.e., a triplexer. The triplexer consists of three series quarter-wavelength transmission lines, three bandpass filters, and three transmission lines for tuning of the filter impedance. The principle of operation is that each sub-band has a matched input impedance ( $50 \Omega$  in this design) at the junction, but a high input impedance at the input of other sub-bands. The series transmission lines of three different quarter wavelengths provide a high impedance at the respective frequency band, i.e., preventing sub-band #1 signals to reach sub-band #2 and #3. The filter tuning lines at the junctions optimize the stop band impedance of each filter, to provide a high stop band impedance in the neighbouring bands. Neighbouring sub-bands are most critical to a sub-band since the band-pass filter has limited rejection close to its pass-band. The entire network is optimized together with the filters to achieve flat passbands and a symmetric performance between the sub-bands (Karlsson et al., 2006; Karlsson & Gong, 2007; Karlsson et al. Nov. 2008).

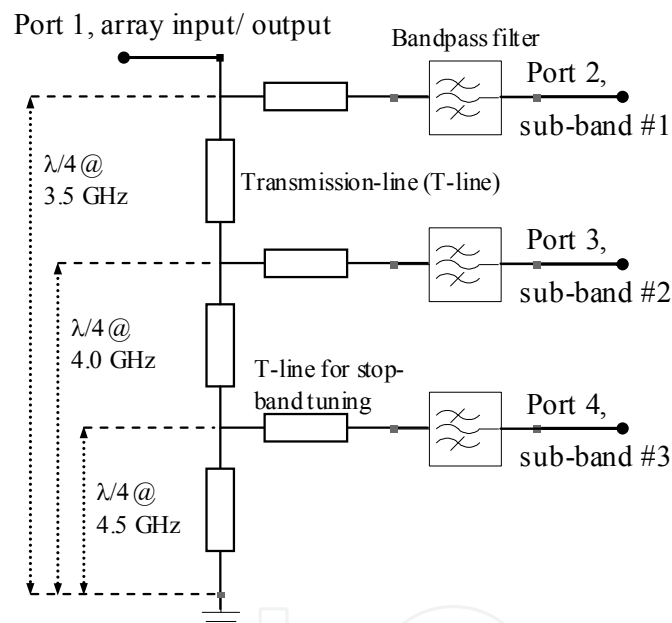


Fig. 5. Triplexer utilizing the manifold principle.

### 4.1 Combined Broadside- and Edge-coupled Filter Technology

Fig. 6(a) and (b) show the broadside-coupling and edge-coupling, respectively. All implementations are made using microstrips. Fig. 6(c) shows the combined broadside- and edge-coupled filter. The start and the stop segments are placed on Metal layer 1 (see Fig. 6(c)), and the rest of the filter is placed on Metal layer 2. A fifth order band-pass filter, two orders from broadside-coupling and three orders from edge-coupling are utilized.

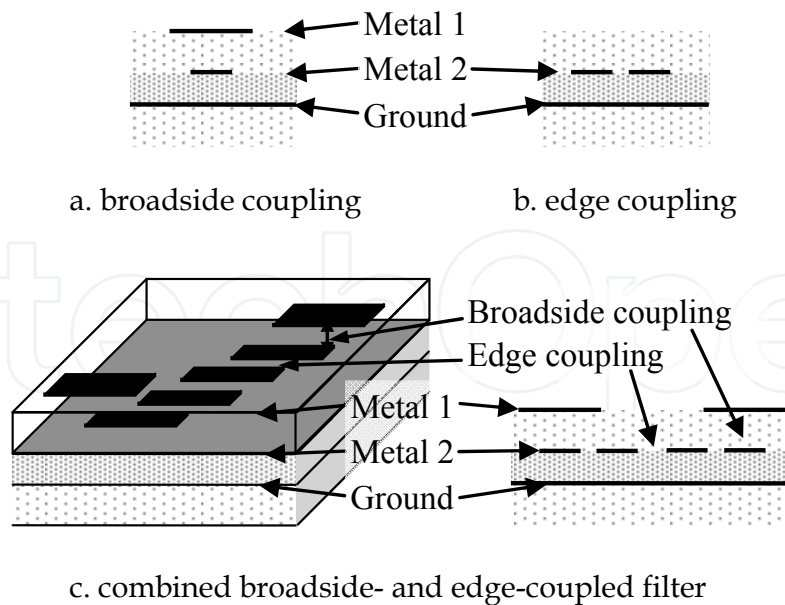


Fig. 6. Filter structures.

#### 4.2 Implementation with Conventional Multi-layer Printed Circuit Board

Fig. 7 shows a photo of the implementation with the substrate shown in Fig. 2(a). The size of the triplexer prototype is 53 x 60 mm. Three of the four soldered Sub-Miniature A (SMA) connectors are seen. SMA connectors mounted from the side connect the three input sub-bands. Port 2 is for sub-band #1 (3.432 GHz), Port 3 is for sub-band #2 (3.960 GHz), and Port 4 is for sub-band #3 (4.488 GHz). The fourth output connector (Port 1) is mounted on the backside of the printed circuit board, i.e., only the soldered signal pin is seen. Moreover, it is

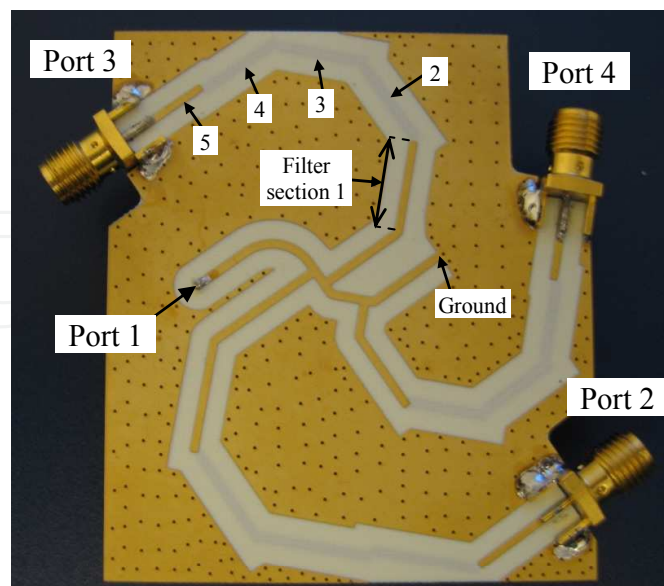
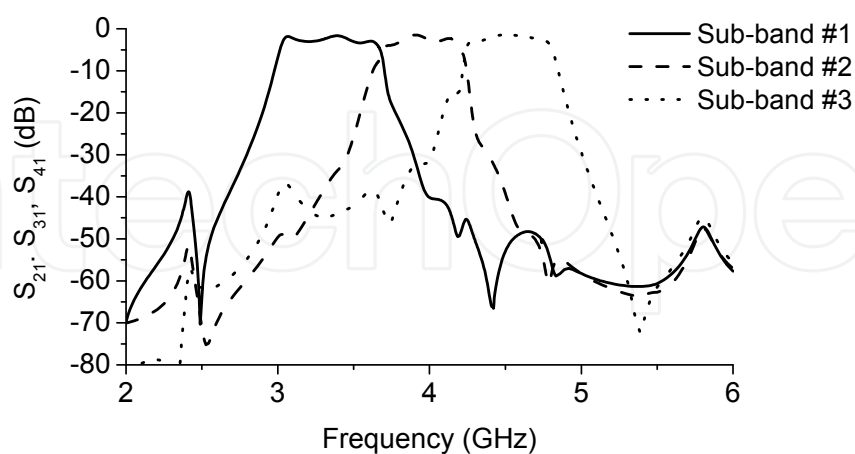


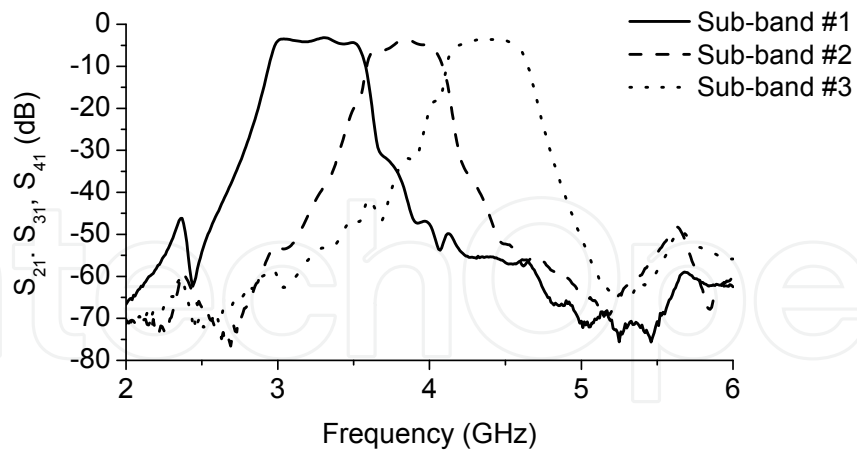
Fig. 7. Photo of the implementation.

seen that the prototype has a bend shape, which was done to achieve a more compact design. The design relies on impedance-controlled microstrip-lines, so the bending has no noticeable effect on the filter characteristic. Design and simulation were done with Advanced Design System (ADS) from Agilent technologies Inc. Measurements were done with a Rhode&Schwartz ZVM vector network analyzer.

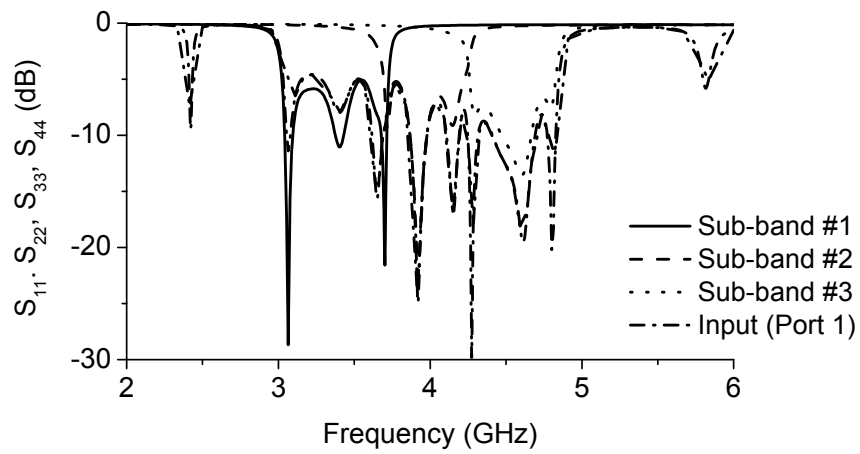
Fig. 8(a) and (b) show the simulation and measurement results of forward transmission of the triplexer, respectively. A fairly flat passband response is seen. The transmission line network is optimized together with the filters to achieve high blocking of neighbouring bands. A good match between simulation and measurement results is seen. The complete multi-layer structure was simulated with radiation characteristics enabled in ADS for the best accuracy. However, some limitations still exist in the simulations. The SMA connectors are not included, and moreover ADS Momentum (ADS electromagnetic simulator) does not take surface roughness into count. The simulated insertion loss is 1.3-1.6 dB, and measured insertion loss is 3.1-3.5 dB for the three sub-bands. All sub-bands have at least 500 MHz bandwidth at -3 dB from the top. Fig. 8(c) and (d) show the simulation and measurement results of return loss of the triplexer, respectively. Due to the narrow guard-band blocking of neighbouring bands a smooth forward transmission was prioritized over low return loss, as seen in Fig. 8(a)-(d). The design freedom to achieve a low return-loss and smooth forward transmission is therefore limited. However, to use higher order than the fifth order band-pass filters would increase the design freedom but losses will increase. Fig. 8(e) and (f) show simulated and measured group delay, respectively. It is seen that for all the 500 MHz sub-bands the group delay is around 3.0 ns and the variation is approximately 1.0 ns within each sub-band. Fig. 8(g) shows isolation between Ports 2-4. It is seen that the minimum isolation is 23 dB. The minimum isolation occurs at the boundary of the neighbouring sub-bands, so in the three passbands the isolation is better than 23 dB. The isolation between the non-neighbouring alternate sub-bands is 51 dB. This work was originally presented in (Karlsson et al. Nov. 2008).



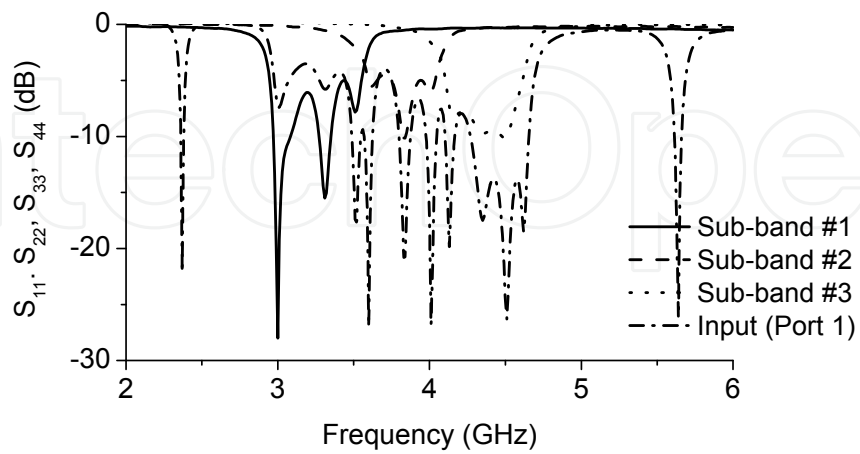
a. simulation of forward transmission



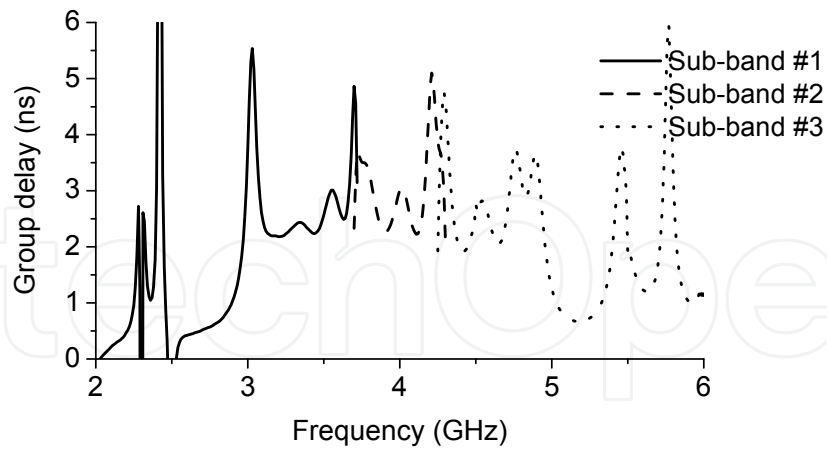
b. measurement of forward transmission



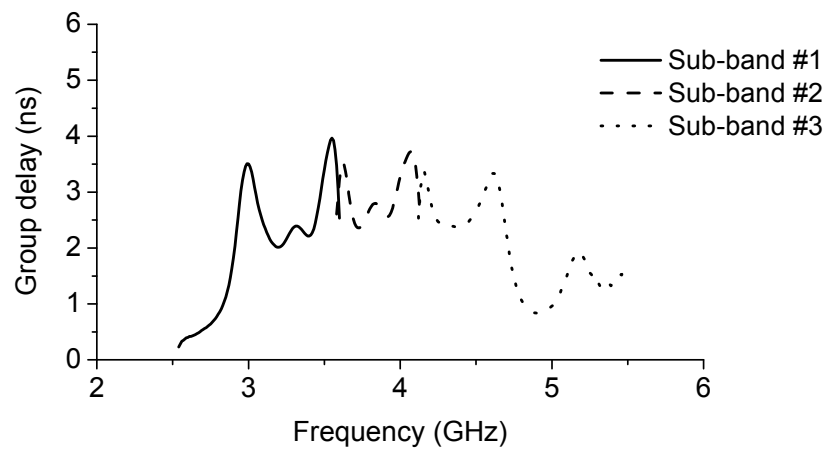
c. simulation of return loss



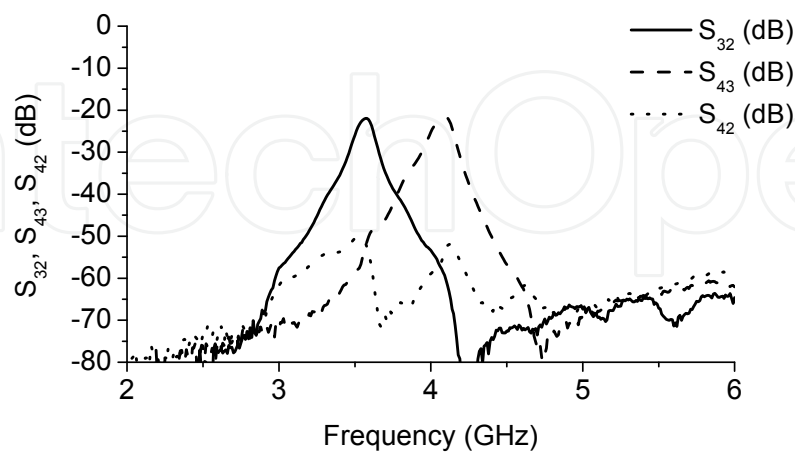
d. measurement of return loss



e. simulation of group delay



f. measurement of group delay



g. measurement of isolation between neighboring and alternate sub-bands

Fig. 8. Triplexer simulations and measurements.

### 4.3 Implementation with the Flex-rigid Substrate

Fig. 9 shows a photo of the implementation with the substrate shown in Fig. 2(b). The network is realized with a microstrip technology in the rigid part. The size of the triplexer prototype is 25 x 48 mm. Three of the four soldered Sub-Miniature A (SMA) connectors are seen. SMA connectors mounted from the side connect the three input sub-bands. Port 1 is the array input/ output (6-9 GHz), Port 2 is for sub-band #1 (6-7 GHz), Port 3 is for sub-band #2 (7-8 GHz), and Port 4 is for sub-band #3 (8-9 GHz).

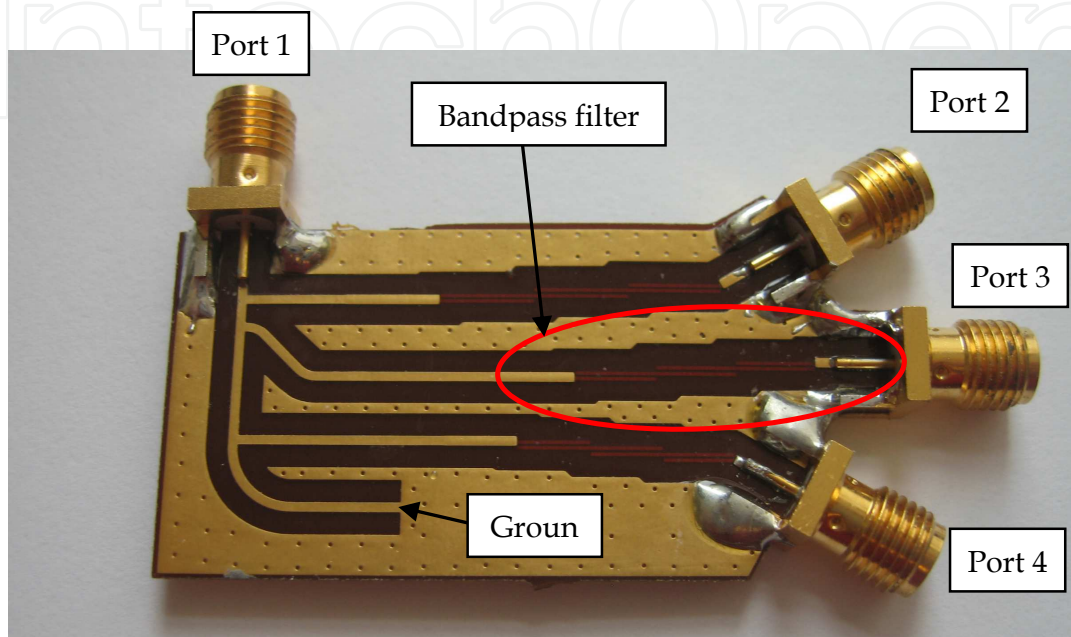
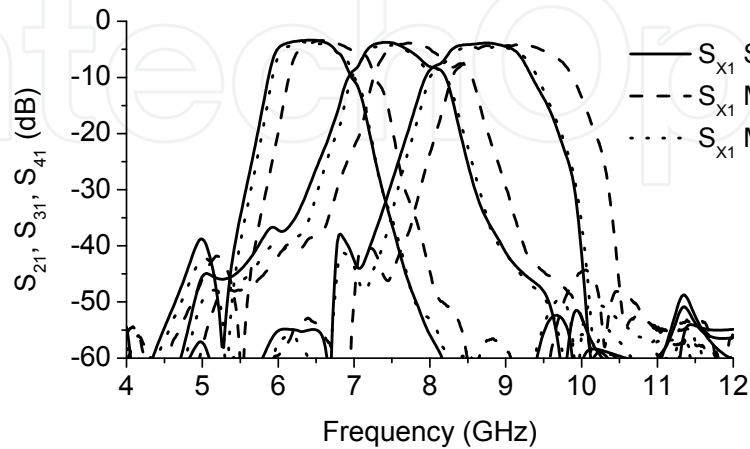


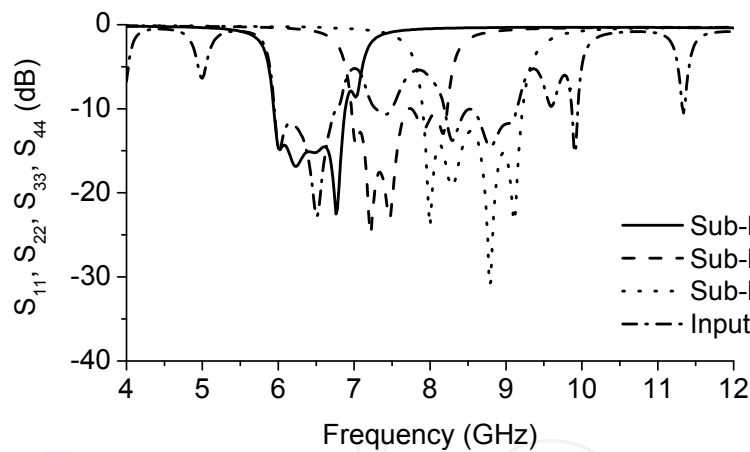
Fig. 9. Triplexer prototype photo.

Fig. 10(a) shows the simulation and measurement results of forward transmission of the triplexer. A fairly flat passband response is seen. The transmission line network is optimized together with the filters to achieve high blocking of neighbouring bands. A good match between simulation and measurement results is seen. The complete multi-layer structure was simulated with radiation characteristics enabled in ADS for the best accuracy. However, some limitations still exist in the simulations. The SMA connectors are not included, and as previously mentioned ADS Momentum does not take surface roughness into count. The simulated insertion loss is 3.35-3.85 dB, and measured insertion loss is 3.41-4.10 dB for the three sub-bands. All sub-bands have at least 1 GHz bandwidth at -3 dB from the top. Fig. 10(b) and (c) show the simulation and measurement results of return loss of the triplexer, respectively. Due to the narrow guard-band blocking of neighbouring bands a smooth forward transmission was prioritized over low return loss, as seen in Fig. 10(a)-(c). However, to use higher order than the fifth order band-pass filters would increase the design freedom but losses will increase. The only noticeable difference is a small frequency shift, due to the fact that the simulated phase velocity likely differs from the actual (Karlsson et al., 2008). Because of that known issue a scaled version of the triplexer was also designed, fabricated and measured, see the dotted line labelled -5 % in Fig. 10(a). The -5 % notation is with respect to frequency, i.e., all electrical lengths were scaled up with 5 %. Fig. 10(d) shows measured isolation between Ports 2-4. It is seen that the minimum isolation is 15 dB. The minimum isolation occurs at the boundary of the neighbouring sub-bands, so in the

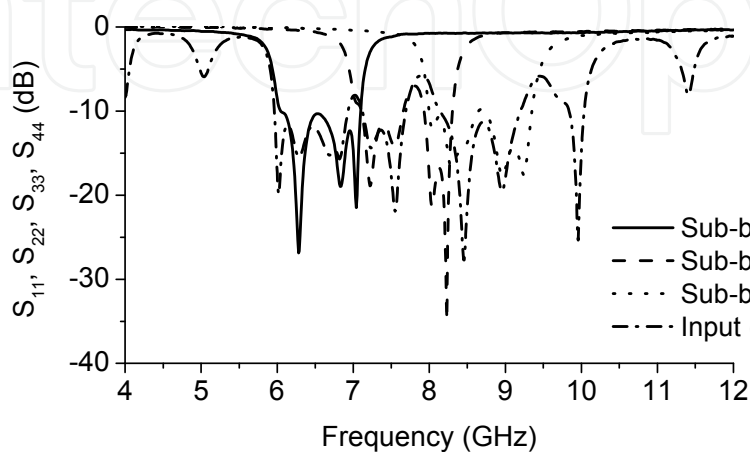
three passbands the isolation is better than 15 dB. The isolation between the non-neighbouring alternate sub-bands is 45 dB. Fig. 10(e) shows measured phase response. It is seen that all three sub-bands have a high degree of linearity within their respective passbands. Fig. 10(f) shows measured group delay. It is seen that for all the 1 GHz sub-bands the group delay is around 1.0 ns and the variation is approximately 0.4 ns within each sub-band. It is the filter type and filter order that dominate the delay (Karlsson et al., 2008).



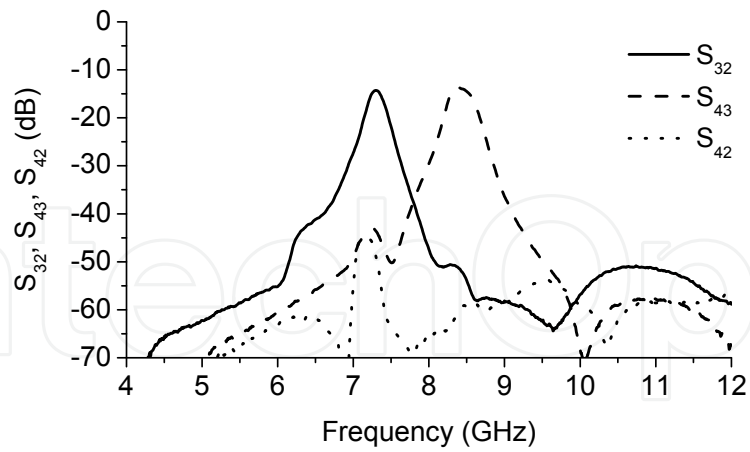
a. simulation and measurement of forward transmission



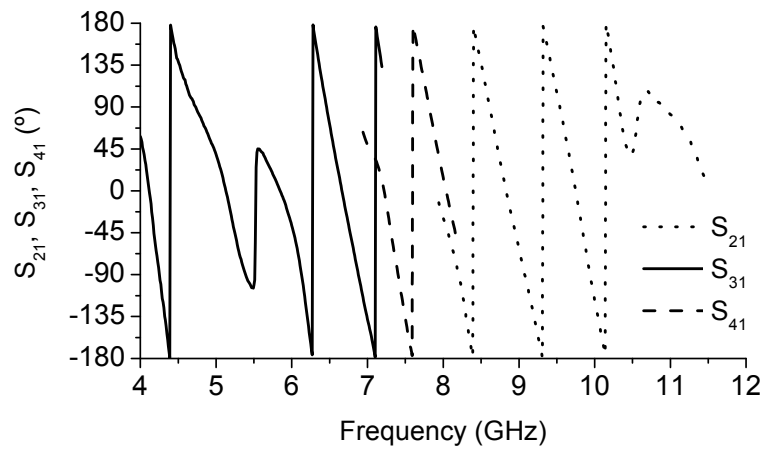
b. simulation of return loss



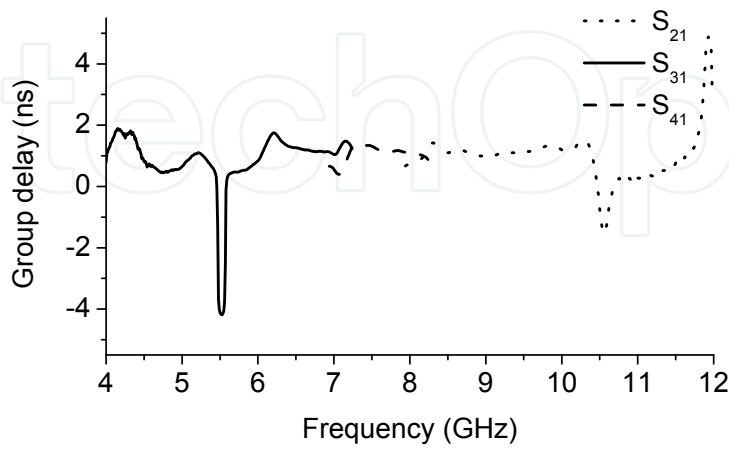
c. measurement of return loss



d. measurement of isolation between neighboring and alternate sub-bands



e. measurement of sub-band phase response



f. measurement of group delay

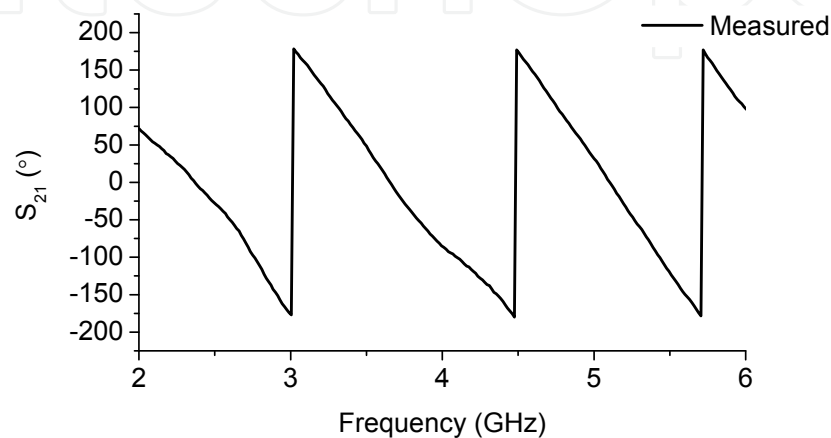
Fig. 10. Triplexer simulations and measurements.

## 5. Radio Front-end

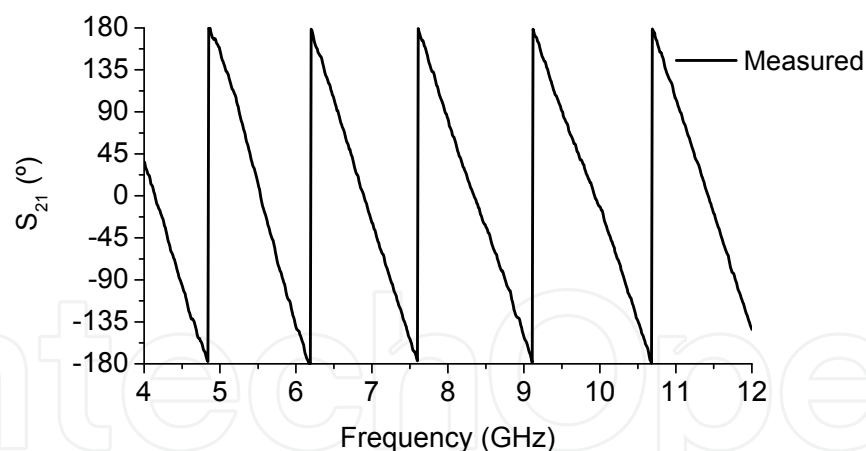
A single wideband antenna is used to transmit three parallel channels (Fig. 5). A suitable wideband antenna can be those presented in Section 3.

### 5.1 Antenna

Fig. 11(a) shows the measured  $S_{21}$  phase response from a transmission between two identical circular dipole antenna (Fig. 3a), including the contribution from one transmitter antenna and one receiver antenna. It is seen that the established radio link has good phase linearity.



a. measurement of phase response, two Mode 1 UWB antenna



b. measurement of phase response, two 6-9 GHz antenna

Fig. 11. Measured  $S_{21}$  phase response (transmission between two circular dipole antenna).

### 5.2 System

Transmission using two antenna plus a triplexer, i.e., to receive three parallel sub-bands is shown in Fig. 12. The triplexer provides equal performance between the three different sub-bands. A wide band signal is received and divided into three parallel sub-bands using the triplexer. Moreover, both the triplexer and the antenna are bi-directional, e.g., suitable for

both transmit and receive operations. For instance, the triplexer can be used to connect one antenna to three parallel transceiver channels or three antenna to one common transceiver.

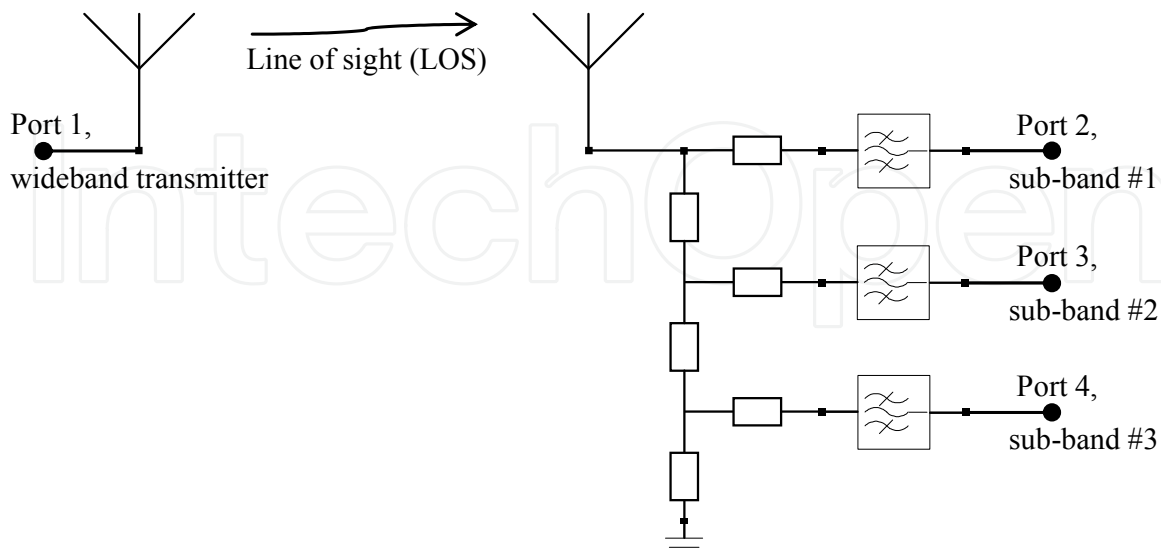


Fig. 12. Measured parallel channel transmission.

In this section a demonstration of a system providing three 500 MHz channels is shown. In theory an arbitrary number of sub-bands, of equal or unequal bandwidth can be combined with manifold multiplexing. The limitations are in general on the actual physical implementation. For instance, the chosen filter topology should be suitable for the actual relative bandwidth. In the design with three equal size sub-bands having almost the same relative bandwidth it is natural to have the same kind of band-pass filter in all sub-bands. Otherwise, it ought to be beneficial to utilize different filter technologies for wide or narrow sub-bands.

During radiation measurements it is important to separate near-field and far-field, i.e., to separate point-dependant electromagnetic coupling from plane wave propagation. The near-far field crossover distance is commonly noted  $R_{ff}$ , see equation 1 (Pozar, 2001). The distance depends on the quote between the largest dimension of the source (upper case  $D$ ) in square and the wavelength ( $\lambda$ );  $c$  and  $f$  are the speed of light in vacuum in metres per second and the frequency in hertz, respectively. If the distance between the transmitting and receiving antenna is larger than  $R_{ff}$ , then it is a far field measurement (Fraunhofer diffraction) and if the measuring distance is less than  $R_{ff}$ , it is a near field measurement (Fresnel zone).

$$R_{ff} = \frac{2D^2}{\lambda} = \frac{2D^2f}{c} \quad (1)$$

Free-space path loss (FSPL) is the loss in signal strength of a propagating wave from a line-of-sight path through free space (Pozar, 2001; Fusco, 2005), assuming that no obstacles nearby causes reflection or diffraction. Moreover, it does not take such factors into count as the gain of the antenna at the transmitter and receiver sides or any loss in the transceiver

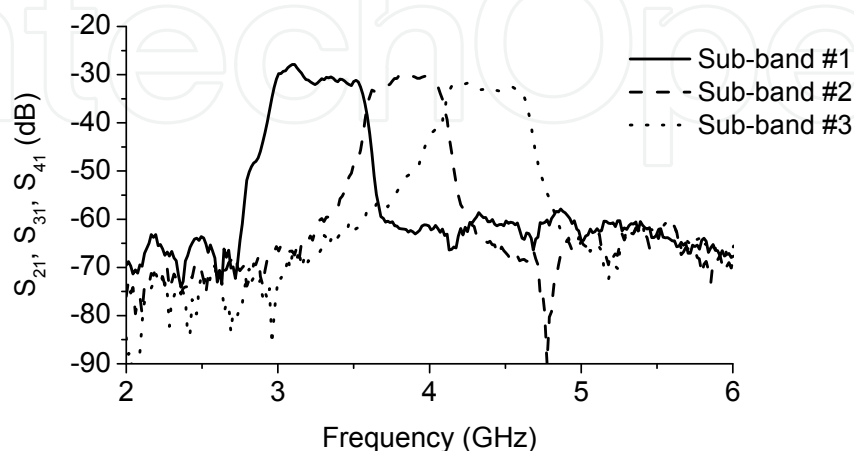
hardware. Lower case  $d$  is the distance between the transmitter and receiver antenna in meters,  $\lambda$ ,  $c$  and  $f$  are defined as above.

$$\text{FSPL} = \left( \frac{4\pi d}{\lambda} \right)^2 = \left( \frac{4\pi d f}{c} \right)^2 \quad (2)$$

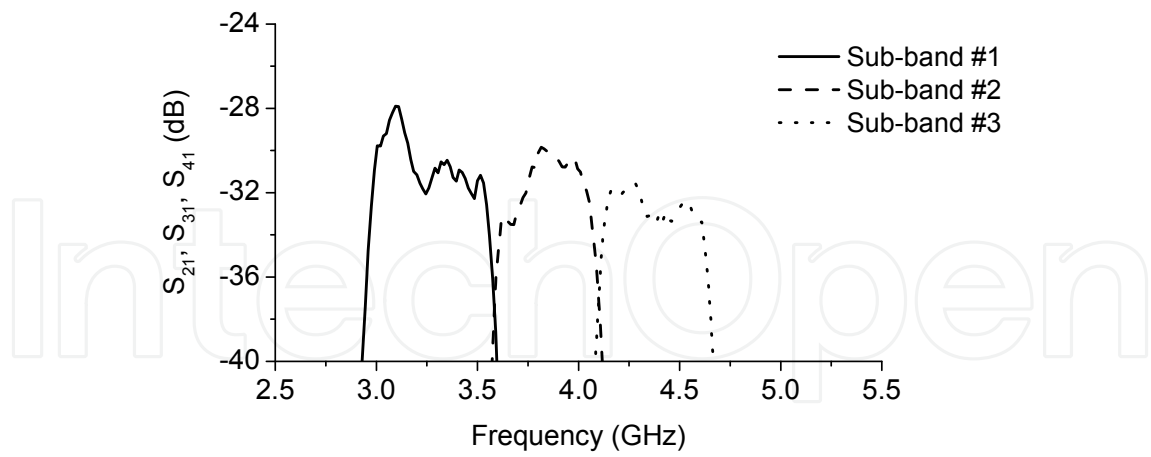
and in decibels (dB):

$$\text{FSPL}_{\text{dB}} = 10 \log_{10} \left( \frac{4\pi d f}{c} \right)^2 \quad (3)$$

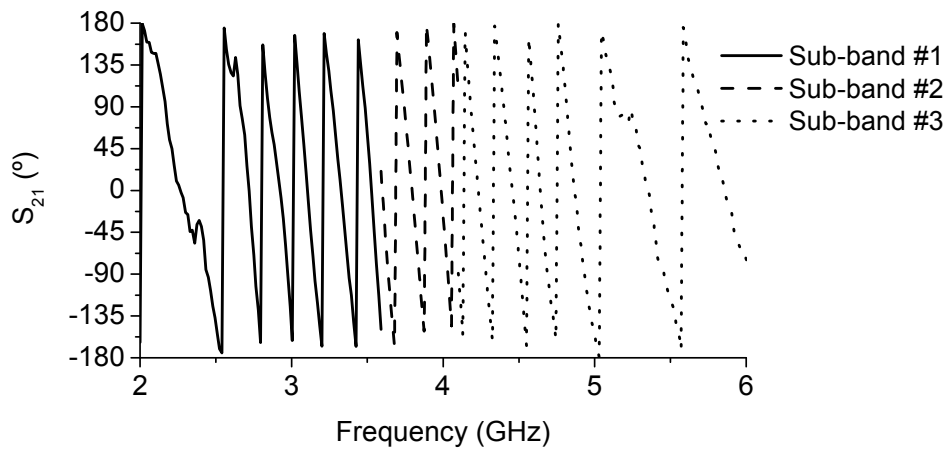
Using equation (1) the maximum  $R_{\text{ff}}$  distance for the “Mode 1 UWB antenna” within the Mode 1 frequency-band is calculated to 4.6 centimetres (cm) at 4.8 GHz. Furthermore, a measurement distance of 20 cm was chosen, which is four times of the maximum  $R_{\text{ff}}$  distance. Using equation (3), the estimated  $\text{FSPL}_{\text{dB}}$  ranges from -28 to -32 dB (from 3.1 to 4.8 GHz). Fig. 13(a) shows the measured results of forward transmission of the front-end. A relatively flat passband response is seen, as expected from the triplexer filter characteristics. Fig. 13(b) shows only the passband, it is seen that all channels have more than 500 MHz bandwidth at -3 dB from the top value within each sub-band. Moreover, it is seen that the three sub-bands have a similar performance. Comparing the sub-bands it should also be considered that the loss contribution due to free space path loss is frequency dependant, i.e., it increases with the square of the frequency. As shown in detail in section 4.2 the measured insertion loss (IL) of the three triplexer sub-bands was measured to be 3.1-3.5 dB, see Fig. 8(b). As shown in section 3 the circular dipole Mode 1 UWB antenna has a simulated and measured gain around 2 dBi, see Fig. 4(c). A coaxial cable with 1 dB loss that was not included in the instrument calibration was used to connect the antenna to the triplexer. Expected  $S_{x1}$  (dB) will then be  $\text{FSPL}_{\text{dB}} + \text{transmitter antenna gain (2 dBi)} + \text{receiver antenna gain (also 2 dBi)} - \text{cable loss (1 dB)} - \text{triplexer IL (3.1-3.5 dB)}$ . Considering antenna gain, losses and the calculated FSPL it is seen that the results in Fig. 13(a) correlates very well with the theoretical expectations. The phase response in Fig. 13(c) shows that all sub-bands have good linearity within their respective frequency ranges, which is also recognized in the low group delay variation seen in the plot, in Fig. 13(d).



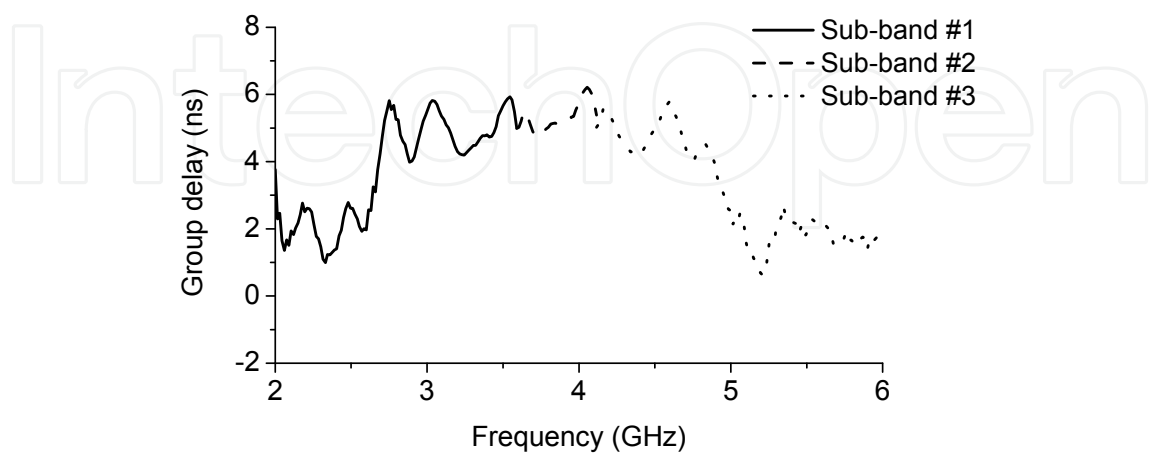
a. measurement of forward transmission of the radio link



b. measurement of forward transmission (pass-band only)



c. measurement of phase response



d. measurement of group delay

Fig. 13. Measured parallel channel transmission.

## 6. Conclusion

A fully integrated planar triplexer using microstrips for multi-band UWB has been presented. Three flat sub-bands in the frequency band 3.1-4.8 GHz and 6-9 GHz for multi-band UWB have been achieved. The triplexer can be integrated into a printed circuit board using a commercial process at low cost, even though the guard-band has only a relative bandwidth of 0.7 % between the three sub-bands. The triplexer uses three filters with a combined broadside- and edge-coupled structure. It is verified that this kind of combined broadside- and edge-coupled filters has higher performance than that of conventional edge-coupled filters.

Two circular dipole antenna with integrated baluns using the flex-rigid substrate can cover the lower UWB frequency band (3.1-4.8 GHz) and the upper UWB band (6-9 GHz) at a measured VSWR around 2. Furthermore, a wide and stable radiation pattern is achieved. Moreover, good phase linearity is observed when the antenna is used in a wireless transmission, i.e., good linearity in both transmitting and receiving operations. With these excellent properties the antenna can be either used as stand-alone components or integrated in a UWB system.

It is shown that using a triplexer and a circular dipole antenna 500 MHz sub-bands can be processed in parallel with equal performance. Moreover, the whole system, i.e., antenna, balun, and triplexer including filters is implemented using only distributed components. The passband shape of the transmitted sub-channels is very close to the shape of the sub-bands in the stand-alone triplexer, indicating that the passband of the filters dominates the shape of the passbands of the transmitted channels. Moreover, a linear phase response and a group delay variation of 1 ns for each transmitted sub-band are obtained.

## 7. References

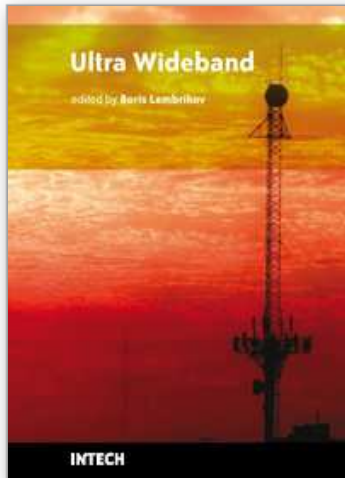
- Coale, F. S. (1958). Applications of Directional Filters for Multiplexing Systems. *Trans. Microwave Theory and Tech.*, Vol. 6, No. 4, pp. 450-453
- Rhodes, J. D. & Levy, R. (1979). A generalized multiplexer theory. *Trans. Microwave Theory and Tech.*, Vol. 27, No. 2, pp. 99-111, Feb. 1979
- Rhodes, J. D. & Levy, R. (1979). Design of General Manifold Multiplexers. *Trans. Microwave Theory and Tech.*, Vol. 27, No. 2, pp. 111-123, Feb. 1979
- Bandler, J. W.; Kellermann, W. & Madsen, K. (1987). A nonlinear  $l_1$  optimization algorithm for design, modeling, and diagnosis of networks. *IEEE Trans. Circuits and Systems*, Vol. 34, No. 2, pp. 174-181, Feb. 1987
- Mansour, R. R. (1994). Design of Superconductive Multiplexers Using Single-Mode and Dual-Mode Filters. *Trans. Microwave Theory and Tech.*, Vol. 41, No. 7, pp. 1411-1418, Jul. 1994
- Rauscher, C. (1994). Efficient design methodology for microwave frequency multiplexers using infinite-array prototype circuits. *Trans. Microwave Theory and Tech.*, Vol. 42, No. 7, pp. 1337-1346, Jul. 1994
- Kirilenko, A. A.; Senkevich, S. L.; Tkachenko, V. I. & Tysik, B. G. (1994). Waveguide duplexer and multiplexer design. *Trans. Microwave Theory and Tech.*, Vol. 42, No. 7, pp. 1393-1396, Jul. 1994

- Matthaei, G. L.; Rohlfing, S. M. & Forse, R. J. (1996). Design of HTS, lumped-element, manifold-type microwave multiplexers. *Trans. Microwave Theory and Tech.*, vol. 44, no. 7, pp. 1313-1321, Jul. 1996
- Bariant, D.; Bila, S.; Baillargeat, D.; Verdeyme, S.; Guillon, P.; Pacaud, D. & Herren, J. J. (2002). Method of spurious mode compensation applied to manifold multiplexer design, in *IEEE MTT-S Int. Microwave Symp. Dig.*, 2002, Vol. 3, pp. 1461-1464
- Ohno, T.; Wada, K. & Hashimoto, O. (2005). Design methodologies of planar duplexers and triplexers by manipulating attenuation poles. *IEEE Trans. Microwave Theory and Tech.*, Vol. 53, No. 6, pp. 2088-2095, Jun. 2005
- Chen, C.-F.; Huang, T.-Y.; Chou, C.-P. & Wu, R.-B. (2006). Microstrip duplexers design with common resonator sections for compact size, but high isolation. *Trans. Microwave Theory and Tech.*, Vol. 54, No. 5, pp. 1945-1952, May 2006
- Cameron, R. I. & Yu, M. (2007). Design of manifold-coupled multiplexers," *Microwave Magazine, IEEE*, vol. 8, no. 5, pp. 46-59, Oct. 2007
- Lai, M.-I. & Jeng, S.-K. (2005) A microstrip three-port and four-channel multiplexer for WLAN and UWB coexistence. *Trans. Microwave Theory and Tech.*, Vol. 53, No. 10, pp. 3244-3250, Oct. 2005
- Mallegol, S.; Coupez J.-P.; Person, C.; Lespagnol, T.; Paquelet, S. & Bisiaux, A. (2006) Microwave (De)Multiplexer for Ultra-Wideband (UWB) Non-Coherent High Data Rates Transceiver, in *Proc. 3rd European Radar Conference, EuRAD 2006*, pp. 346-349
- Stadius, K.; Rapinoja, T.; Kaukovoori, J.; Ryyanen, J. & Halonen, K. A. I. (2007). Multitone Fast Frequency-Hopping Synthesizer for UWB Radio. *Trans. Microwave Theory and Tech.*, Vol. 55, No. 8, pp.1633-1641, Aug. 2007
- Tarng, S.-H.; Tsai, Y.-C.; Shen, Y.-S. & Jou, C. F. (2007) A Signal Generator for MB-OFDM UWB System in 0.18  $\mu\text{m}$  CMOS Process, in *IEEE MTT-S Int. Microwave Symp.*, 2007, pp. 2157-2160
- Galbraith, C.; Rebeiz, G. M. & Drangmeister, R. (2007) A Cochlea-based Preselector for UWB Applications, in *IEEE Radio Frequency Integrated Circuits (RFIC) Symp.*, 2007, pp. 219-222
- Karlsson, M. & Gong, S. (2008) Monopole and Dipole Antenna for UWB Radio Utilizing a Flex-rigid Structure, *ISAST Transactions on Electronics and Signal Processing*, Vol. 2, No. 1, pp. 59-63, 2008
- Karlsson, M.; Osth, J.; Owais; Serban, A. & Gong, S. (2009) Circular dipole antenna for lower and upper UWB bands with integrated balun, *IEEE International Conference on Ultra-Wideband, ICUWB 2009*, pp.658-663, 9-11 Sept. 2009
- Karlsson, M. & Gong, S. (2009) Circular Dipole Antenna for Mode 1 UWB Radio with Integrated Balun Utilizing a Flex-rigid Structure, *IEEE Trans. Antenna and Propag.*, Vol. 57, No. 10, pp. 2967-2971, Oct. 2009
- Karlsson, M.; Håkansson, P.; Huynh, A. & Gong, S. (2006) Frequency-multiplexed Inverted-F Antenna for Multi-band UWB, *IEEE Wireless and Microwave Conf. 2006*, pp. 2.1-2.3, 2006
- Karlsson, M. & Gong, S. (2007) A Frequency-Triplexed Inverted-F Antenna System for Ultra-wide Multi-band Systems 3.1-4.8 GHz, *ISAST Transactions on Electronics and Signal Processing*, Vol. 1, No. 1, pp. 95-100, 2007

- Karlsson, M.; Håkansson, P. & Gong, S. (2008) A Frequency Triplexer for Ultra-Wideband Systems Utilizing Combined Broadside- and Edge-Coupled Filters, *IEEE Trans. on Advanced Packaging*, Vol. 31, No. 4, pp. 794-801, Nov. 2008
- Pozar, D. M. (2001) *Microwave and RF Design of Wireless Systems*, John Wiley & Sons Inc., ISBN 0-471-32282-2, USA, 2001
- Fusco, V. F. (2005) *Foundations of Antenna Theory and Techniques*, Pearson Education Limited, Edinburgh Gate, Harlow, Essex, England, ISBN 0-130-26267-6, 2005

IntechOpen

IntechOpen



## **Ultra Wideband**

Edited by Boris Lembrikov

ISBN 978-953-307-139-8

Hard cover, 458 pages

**Publisher** Sciyo

**Published online** 17, August, 2010

**Published in print edition** August, 2010

Ultra wideband technology is one of the most promising directions in the rapidly developing modern communications. Ultra wideband communication system applications include radars, wireless personal area networks, sensor networks, imaging systems and high precision positioning systems. Ultra wideband transmission is characterized by high data rate, availability of low-cost transceivers, low transmit power and low interference. The proposed book consisting of 19 chapters presents both the state-of-the-art and the latest achievements in ultra wideband communication system performance, design and components. The book is addressed to engineers and researchers who are interested in the wide range of topics related to ultra wideband communications.

### **How to reference**

In order to correctly reference this scholarly work, feel free to copy and paste the following:

Magnus Karlsson, Allan Huynh and Shaofang Gong (2010). Parallel Channels Using Frequency Multiplexing Techniques, Ultra Wideband, Boris Lembrikov (Ed.), ISBN: 978-953-307-139-8, InTech, Available from: <http://www.intechopen.com/books/ultra-wideband/parallel-channels-using-frequency-multiplexing-techniques>

**INTECH**  
open science | open minds

### **InTech Europe**

University Campus STeP Ri  
Slavka Krautzeka 83/A  
51000 Rijeka, Croatia  
Phone: +385 (51) 770 447  
Fax: +385 (51) 686 166  
[www.intechopen.com](http://www.intechopen.com)

### **InTech China**

Unit 405, Office Block, Hotel Equatorial Shanghai  
No.65, Yan An Road (West), Shanghai, 200040, China  
中国上海市延安西路65号上海国际贵都大饭店办公楼405单元  
Phone: +86-21-62489820  
Fax: +86-21-62489821

© 2010 The Author(s). Licensee IntechOpen. This chapter is distributed under the terms of the [Creative Commons Attribution-NonCommercial-ShareAlike-3.0 License](#), which permits use, distribution and reproduction for non-commercial purposes, provided the original is properly cited and derivative works building on this content are distributed under the same license.

IntechOpen

IntechOpen